JOURNAL OF MASS SPECTROMETRY, VOL. 32, 461–474 (1997)

SPECIAL FEATURE: TUTORIAL

Slow Heating Methods in Tandem Mass Spectrometry

Scott A. McLuckey* and Douglas E. Goeringer
Chemical and Analytical Sciences Division, Oak Ridge National Laboratory, Oak Ridge, TN 37831-6365, USA

Several approaches to ion activation in tandem mass spectrometry have been developed in recent years for use in ion trapping instruments that allow for conditions to be reached wherein rates of ion activation and deactivation are comparable. These approaches are defined as slow heating methods and include continuous-wave laser infrared multiphoton dissociation, dissociation driven by blackbody radiation, quadrupole ion trap collisional activation and sustained off-resonance irradiation in ion cyclotron resonance mass spectrometry. In the limiting case in which ion activation and deactivation rates are equal, a steady-state parent ion internal energy distribution is achieved and the kinetics of dissociation can be interpreted in analogy with thermal dissociation. This discussion describes the thermal analogy and the limiting conditions of rapid energy exchange and slow energy exchange along with the possible ramifications for dissociation rates and product ion spectra. The figures of merit that the various slow heating methods share as a class of activation methods are also discussed. The purpose of this perspective is to provide a frame-of-reference from which slow heating methods can be considered. Such methods are seeing increasing use as the number of ion trapping instruments grows and have shown remarkable success with dissociation of high-mass ions. © **1997 by John Wiley & Sons, Ltd.**

J. Mass Spectrom. **32**, 461–474 (1997)
No. of Figs: 6 No. of Tables: 0 No. of Refs 113

KEYWORDS: tandem mass spectrometry; slow heating methods; collisional activation; multiphoton dissociation; ion cyclotron resonance; quadrupole ion trap

INTRODUCTION

Next to ionization, the most important reaction in mass spectrometry is unimolecular dissociation. Fragmentation is generally the means by which mass spectrometry can provide information about ion structure which, in turn, often allows for inferences regarding the identity and structure of the neutral species from which the ion was derived. The fragmentation of organic ions that takes place as a result of bombardment of neutral species by 70 eV electrons (electron ionization), for example, is the basis for the identification of unknowns in the widely used technique of gas chromatography/mass spectrometry.[1,2] In this case, the excess internal energy required to induce fragmentation at rates within the time-scale of the instrument is deposited in concert with the ionization event. In tandem mass spectrometry,[3,4] on the other hand, the ionization reaction and activation of an ion of interest are discrete events. Hence, a variety of approaches to ion activation have been explored over the past nearly three decades since tandem mass spectrometry began development as an analytical tool.

The first activation method used in tandem mass spectrometry was kiloelectronvolt (laboratory frame of reference) collisions of ions with a stationary (thermal energy) gaseous target[5–7] wherein single collisions were most likely. Since then, a remarkably wide variety of techniques and conditions have been reported for activating polyatomic ions. The current diversity in activation methods and conditions was motivated by a variety of factors. In some cases, new forms of instrumentation for tandem mass spectrometry mandated novel means for activation. The triple quadrupole tandem mass spectrometer,[8,9] for example, led to the use of relatively low laboratory energy collisional activation largely as a result of the ion kinetic energy requirement for optimal quadrupole mass analysis. Similarly, collisional activation in an ion cyclotron

* Correspondence to: S. A. McLuckey.
This work was sponsored by the Office of Basic Energy Sciences, U.S. Department of Energy, under Contract DE-AC05-96OR22464 with Oak Ridge National Laboratory, managed by Lockheed Martin Energy Research Corp.

CCC 1076–5174/97/050461–14 $17.50

Received 25 February 1997
Accepted 25 February 1997

resonance instrument[10] usually takes place via relatively low-energy collisions owing to limitations in storage of kiloelectronvolt kinetic energy ions. In some cases, new activation methods have been developed directly as a result of deficiencies of established activation methods in leading to structural information. Surface-induced dissociation[11] and electron-induced dissociation[12] are two such examples of activation methods that have been explored as means for overcoming limitations of collisional activation with gaseous targets. Finally, some activation methods for analytical mass spectrometry have grown from techniques used in the ion chemistry community. For example, many of the photodissociation techniques have roots in experiments designed to probe fundamental aspects of unimolecular dissociation.[13–16]

The differentiation of isomeric ion structures was an early motivation for the development and use of ion activation techniques. Since then, mixture analysis, targeted compound detection and biopolymer sequencing have also become applications that drive interest in activation methods. In comparing and contrasting competing methods, the following set of figures of merit are applied:

1. The amount of energy that can be deposited into the ion;
2. The distribution of energies deposited;
3. How readily the deposited energy can be varied;
4. How readily the reaction can be driven, as determined by factors such as cross-section (or rate constant), number density and spatial overlap;
5. The form in which energy is deposited, viz. electronic or vibrational;
6. The time over which activation occurs relative to the time-frame for unimolecular reactions.

The sixth characteristic is the one that is used here to distinguish between fast and slow activation methods. Fast activation methods are those in which the activation event is fast relative to typical time-frames for unimolecular reactions. Clearly within this category are activation events that take place faster than or on the time frame of a vibrational period, such as a single collision at high relative velocity and single UV or visible photon absorption. An intermediate case is that of a "sticky' or orbiting collision in which a relatively long-lived collision complex is formed[17] that may survive for many vibrations prior to breakup. Slow activation methods rely on multiple discrete activation events such as multiple collisions or multiple photon absorption. In these cases, the times between activation events can be long, of the order of microseconds or longer, relative to time-frames for unimolecular chemistry. Therefore, reactions can occur during the course of the activation process. This overview is focused on 'very slow' activation methods, referred to herein as slow heating methods, which are distinguished from 'slow' activation methods by the fact that deactivation processes (e.g. cooling collisions or photon emission) occur during the activation period, in competition with activation.

The purpose of this overview is to bring attention to the increasing use of slow heating methods in analytical mass spectrometry and to highlight the various techniques with emphasis on their commonalities that distinguish them from faster activation techniques. Several of these methods could themselves be the subject of a lengthy review. The aim here, however, is simply to provide a description of how each method works and how it fits into the overall picture with respect to slow heating of ions in tandem mass spectrometry (MS/MS). Specifically, we discuss collisional activation methods, such as sustained-off-resonance-irradiation[18] (and related techniques) in ion cyclotron resonance mass spectrometry, quadrupole ion trap collisional activation[19] and radiation-based techniques such as continuous-wave infrared laser multiphoton dissociation,[20] and dissociation driven by the absorption of blackbody radiation.[21] The activation figures of merit are discussed further below, to provide a context within which slow heating methods can be considered with respect to other forms of ion activation, followed by a discussion of the characteristics of slow heating including the important limiting case in which heating and cooling rates are equal. The figures of merit of slow heating methods are then discussed followed by brief descriptions of the aforementioned slow heating methods.

ACTIVATION FIGURES OF MERIT

The various figures of merit for an ion activation method are elaborated upon more fully in this section to provide a context within which fast, slow and very slow (slow heating) activation methods can be considered. It is important to recognize, however, that the relative importance of each figure of merit is application dependent. It is for this reason, in part, that so many forms and variations of activation methods are in use.

The magnitudes and distribution of energies that can be deposited into an ion, the first two figures of merit mentioned above, are of obvious importance owing to their roles in determining the identities and abundances of product ions resulting from ion activation.[22] The most structurally informative dissociation channels are not always those of lowest critical energy. It is therefore desirable to be able to deposit sufficient energy to access the dissociation channels of greatest interest. Furthermore, for particularly stable ions and for those with many degrees of freedom, large energy transfers may be necessary to drive decomposition at sufficiently high rates for the time-scale of the MS/MS experiment. In some activation methods, such as UV photodissociation, the distribution of energies deposited into the ion is very narrow and the magnitude is well defined, whereas in others, such as keV (lab) collision energy collisional activation, the energy transfer distribution tends to be quite broad and ill-defined.[23]

The third figure of merit relates to the variability of the above parameters (viz. energy magnitude and distribution). Given the extremely wide range of parent ion types that can be subjected to ion activation in an MS/MS experiment, ranging from diatomic ions to large biopolymers and from relatively loosely bound species to those with high stabilities, it is clearly desirable to be able to vary the magnitude and, possibly, the shape of the energy transfer distribution associated with ion activation. The facility with which this can be done

varies with the activation method and, sometimes, with the experimental conditions. For example, significant changes in product ion spectra resulting from collisional activation can often be observed as a result of changing collision energy in the low (5–100 eV) collision energy regime,[24] whereas spectra derived from keV energy collisional activation tend to be less sensitive to changes in collision energy.[4]

The fourth figure of merit (i.e. efficiency) is particularly important for analytical applications in that it deals with the cost, in terms of sensitivity and detection limits, associated with the gains in specificity and new information afforded by the MS/MS experiment. While instrumental factors can play a major role in determining the fraction of parent ions that are converted into detected product ions, the physics and chemistry of the activation reaction and any competing processes are also important. In beam-type experiments employing collisional activation with a gaseous target, it is usually most convenient to consider the activation reaction in terms of a Beer's law relationship such as

$$[M_p^+] = [M_p^+]_0 e^{-n\sigma l} \quad (1)$$

where $[M_p^+]_0$ represents the parent ion flux in the absence of the target gas, $[M_p^+]$ is the parent ion flux after introduction of the target gas, l is the pathlength, n is the target number density and σ is the total ion loss cross-section. In the absence of losses other than by dissociation, σ represents the cross-section for collisional activation leading to dissociation, otherwise commonly referred to as the cross-section for collision-induced dissociation, σ_{CID}. In ion trapping instruments, it is often more convenient to consider collisional activation between stages of mass analysis in terms of rate constants and reaction times, viz.

$$[M_p^+]_t = [M_p^+]_0 e^{-nkt} \quad (2)$$

where $[M_p^+]_t$ represent the unreacted parent ion population after reaction time t, $[M_p^+]_0$ is the parent ion population prior to reaction and k is the rate constant for all ion loss processes. In the absence of any ion loss processes other than dissociation, k is simply the rate constant for collision-induced dissociation, k_{CID}.

For most forms of ion activation, expressions analogous to Eqn (1) or (2) can be written and are useful in considering the extent to which parent ions can be converted to product ions under the available experimental conditions. Ideally, all of the mass-selected parent ions can be converted into informative product ions. This rarely occurs in practice but, as will be discussed further below, it is most likely to occur in ion trapping instruments using a slow or very slow activation method. This follows from the ability to vary reaction time over several orders of magnitude in most ion trapping instruments. In beam-type instruments, the only variable in Eqn (1) available to the experimentalist is n, the target number density. A positive correlation between absolute product ion yield and n may hold over a range of n but eventually other ion loss processes, most notably scattering, tend to dominate. In ion trapping instruments, on the other hand, conversion of parent ions to product ions can be altered either by increasing n, thereby increasing the reaction rate as given by the product of n and k, or by increasing t, the reaction time. Therefore, it is often straightforward in ion trapping instruments to increase the conversion of parent ion to product ions by increasing reaction time so as to avoid any deleterious effects associated with increasing the target number density. An analogous measure in beam-type instruments would be to vary the pathlength (i.e. the length of the collision region), which is not ordinarily straightforward. However, it is important to recognize that beyond the point at which zero or one activation event is most likely, increasing reaction time or target number density increases the probability of multiple activation events. For typical cross-sections associated with collisions or photon absorption, high conversion efficiencies can only be obtained via multiple activation events, which implies a slow or very slow activation method.

The fifth characteristic is included to account for situations in which the ion may not behave statistically.[25] That is, for example, in cases in which fragmentation from an excited electronic state is faster than conversion to excited vibrational levels of the electronic ground state, in violation of the usual assumption in statistical theories of mass spectra[26–28] that internal energy equilibration is fast relative to fragmentation rates. In these cases, product ion spectra derived from activation methods that initially deposit energy via promotion of the ion to an excited electronic state versus those that directly induce vibration in the electronic ground state can lead to different fragmentation behavior for reasons other than differences in the energy transfer distribution. An elegant example of such a situation has recently been described by Shukla *et al.*[29] for ionized acetone using collisional activation under different collision energy conditions.

The sixth characteristic listed above for an activation method distinguishes between fast and slow activation methods. If chemistry can occur during the activation process, such as rearrangement or fragmentation, the activation process is classified as being 'slow'. This ordinarily implies multiple activation events spaced over a time period that is long with respect to unimolecular reaction rates. A wide variety of conditions in mass spectrometry has been used to induce dissociation via slow activation. These include collisional activation in beam-type tandem mass spectrometers using target number densities that give rise to multiple collisions[30–37] and dissociation in the atmosphere/vacuum interface in electrospray ion sources (e.g. nozzle–skimmer dissociation[38]). Slow heating methods, which involve both ion heating and ion cooling steps during the activation period, include thermal heating at near atmospheric pressure in an electrospray ion source[39,40] (not an MS/MS experiment), and the slow heating methods mentioned in the Introduction and discussed further below.

CHARACTERISTICS OF SLOW HEATING METHODS

For the purpose of this overview, we have categorized activation methods as being either fast, slow or very slow. In reality, the various approaches to ion activation fall on a scale ranging from activation that takes

place on the time-scale of electron motion, as in UV photodissociation, to very slow heating methods, wherein Boltzmann statistics can be applied. Reviews of photodissociation have generally covered both single and multiphoton absorption situations.[13–16,41–44] Most reviews of collisional activation, using either gaseous targets[45–54] or a solid surface target,[55,56] on the other hand, have largely addressed single collision dynamics. The dynamics of single activation events obviously also apply to slow and very slow activation methods. However, the fact that very slow activation methods involve multiple discrete activation events that occur over an extended period of time allows for other processes, such as deactivation events, rearrangements and sequential fragmentation reactions, to affect the product ion spectrum. Even among the slow and very slow activation methods, there is significant variation in experimental conditions that can make for subtle but significant differences in the appearance of product ion spectra derived therefrom. These differences include, for example, the average time between activation/deactivation events, the magnitudes of energy gain/loss and the rates at which reactions are driven.

While there can be significant variation in the mechanisms and conditions for energy transfer among the various activation methods, it is instructive to classify them on the basis of activation time. Figure 1 shows a time-scale ranging from 10^{-16} to 10^{3} s, which represents the time range for activation methods currently being used in tandem mass spectrometry. The time over which activation occurs with various commonly used activation methods is indicated to the right of the time-scale. At short times, activation is bounded by the fastest chemical events, viz. those based on electron motion. Since the time associated with the orbital motion of a valence electron is about 10^{-15} s, ion activation cannot occur much faster than this without recourse to excitation of core electrons. At long times, practical considerations, such as ion storage efficiencies and analysis times, become limiting factors.

In considering Fig. 1, it is important to distinguish between activation time, as indicated in the figure, and the time associated with a single activation event during an activation process. In the case of activation by a single event, as in UV photodissociation effected under conditions in which the probability of the absorption of two or more photons is low, or in collisional activation under single collision conditions, the single activation event constitutes the entire activation process. The activation time and the time for the activation event are the same. However, when activation involves multiple activation events, the activation process is generally far longer than the individual activation events that make up the process. Single-event activation processes, such as collisional activation on a surface or with a gas and activation by absorption of a single photon, are therefore the fastest methods for ion activation. For cases in which multiple activation events are likely, the time for

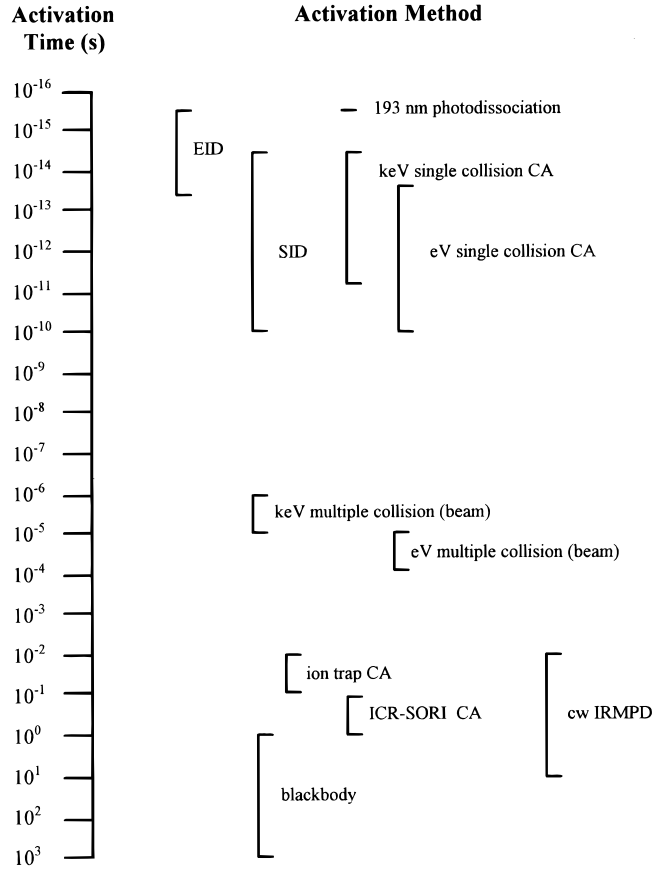

Figure 1. Typical ranges of activation times associated with various activation methods in tandem mass spectrometry. EID = electron-induced dissociation; SID = surface-induced dissociation; CA = collisional activation; (beam) = typical conditions used in a beam-type tandem mass spectrometer; ICR-SORI = ion cyclotron resonance sustained off-resonance irradiation; cw IRMPD = continuous wave infrared multiphoton dissociation.

the activation process spans the entire period over which excitation events can occur. In the case of collisional activation in a beam-type instrument operated with target gas pressures sufficiently high that multiple collisions are likely, the time of the activation process is equal to the time the ion takes to pass through the collision region. In the case of photodissociation using power levels sufficiently high that multiphoton absorption is likely, the time of the activation process is equal to the pulse length. The two examples just given constitute activation processes of intermediate length. In the latter case, nanosecond laser pulses are commonplace[15,57–59] whereas collisional activation under multiple collision conditions in a beam-type tandem mass spectrometer occurs over a time of the order of ten microseconds. This discussion is focused on methods that employ activation periods in excess of $\sim 10^{-2}$ s.

Very slow activation methods are being used increasingly, in large part owing to the growth in the use of ion trapping instrumentation, most notably quadrupole ion trap and the ion cyclotron resonance instruments. While there are significant differences in the various forms of slow heating, in the limiting case, they all tend to lead to an ion population with either a Boltzmann internal energy distribution or a truncated Boltzmann distribution.[60] For this reason, it is instructive to review briefly unimolecular dissociation kinetics under thermal conditions.

Competition between excitation and de-excitation events in a slow heating method results in a distribution of parent ion internal energies. For the limiting cases in which excitation/de-excitation rates far exceed the unimolecular dissociation rate, the distribution is Boltzmann for a polyatomic ion and the parent ion population can be described as having an internal temperature, $T_{internal}$. In the other limiting case (i.e. the unimolecular dissociation rate is much greater than exitation/de-excitation rates), the high-energy tail of the distribution above the dissociation energy, E_0, is perturbed resulting in a truncated Boltzmann distribution (see below). Distributions between these two limiting cases result when the unimolecular dissociation rate and excitation/de-excitation rates are comparable. A qualitative picture for the evolution of the parent ion internal energy distribution arising from a very slow activation method is illustrated in Figure 2, assuming the parent ion population to have an initial distribution of relatively low internal energies ($T_{internal}$ = 298 K curve) at activation time t = 0. Initiation of ion activation, either by collisional activation or photon irradiation, results in a situation in which the probability of an excitation event exceeds that of a de-excitation event. As long as this situation prevails, the parent ion internal energy distribution shifts to higher energies. Eventually, a steady-state condition is achieved in which the excitation and de-excitation rates are equal and the parent ion population is characterized by a higher $T_{internal}$ ($T_{internal}$ = 500 K curve). Provided the high-energy tail of the distribution exceeds E_0 to an extent that a measurable rate of fragmentation can be observed, a product ion spectrum can be obtained. The following development discusses in somewhat more detail the factors determining the observed rate of parent ion dissociation when the ion population reaches a steady-state condition.

In the general case, the kinetic scheme for thermal unimolecular reactions is

$$AB^+ \underset{k_{-c}[M]+k_{-r}}{\overset{k_c[M]+k_r}{\rightleftharpoons}} AB^{+*} \xrightarrow{k_{uni}} A^+ + B \qquad (3)$$

where AB^+ is the parent ion, AB^{+*} is the activated parent ion, A^+ and B are the ionic and neutral fragments, respectively, $k_c[M]$ is the collisional activation rate involving collision partner M, k_r is the photon absorption rate, $k_{-c}[M]$ is the collisional deactivation rate and k_{-r} is the photon emission rate. A delay time exists between ion activation (i.e. when sufficient internal energy for dissociation has accumulated in the parent ion) and dissociation during which deactivation by another collision can occur, so that $[AB^{+*}]$ reaches a steady-state. Therefore, the observed fragment ion formation rate, $d[A^+]dt = k_{diss}[AB^+]$, depends on the

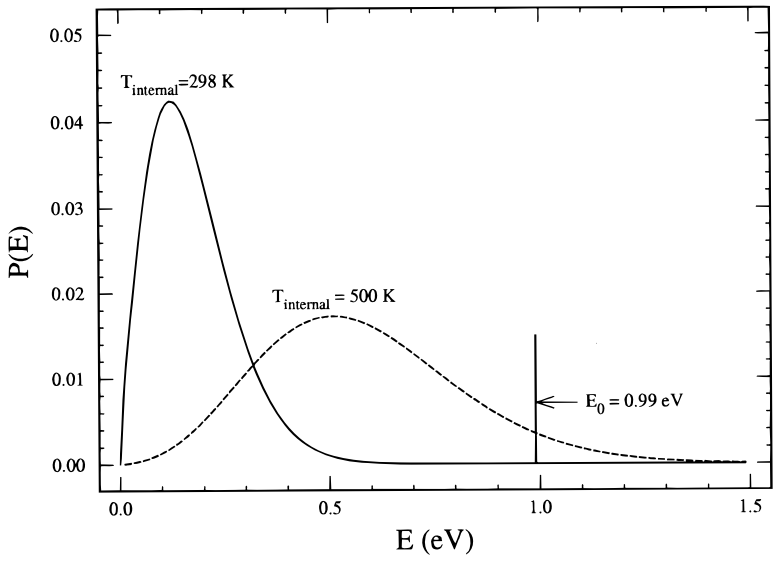

Figure 2. Hypothetical parent ion internal energy distributions for a parent ion population prior to ion activation ($T_{internal}$ = 298 K) and after parent ions have reached the steady-state condition ($T_{internal}$ = 500 K) while undergoing a slow heating activation process.

relative values of the activation rates, the deactivation rates, and the unimolecular dissociation rate constant, k_{uni}, as shown in the equation 4.

$$k_{diss} = \frac{k_{uni}(k_c[M] + k_r)}{k_{-c}[M] + k_{-r} + k_{uni}} \quad (4)$$

Figure 3 shows a plot of log k_{diss} versus log [M] for $k_{uni} = 10^6$ s^{-1}, k_c and $k_{-c} = 10^{-9}$ cm^3 molecule^{-1} s^{-1} and k_r and $k_{-r} = 10$ s^{-1}. While in practice several of these rates are energy dependent (see below), Figure 3 shows qualitatively the expected dependence of k_{diss} on [M] for the common situation in which k_{uni} exceeds k_r and k_{-r}.

It is instructive to consider the limiting cases in which the activation and deactivation rates greatly exceed the unimolecular dissociation rate and vice versa. This is done within the context of the Lindemann theory of thermal unimolecular reactions,[61,62] which ignores photon absorption and emission. However, generalization of the following development to include photon absorption/emission is straightforward. In the Lindemann theory, an equilibrium condition is reached when the collisional excitation and relaxation rates significantly exceed k_{uni}, so that

$$k_{diss} = \frac{k_{uni}\,k_c[M]}{k_{-c}[M]} = k_{uni}\frac{k_c}{k_{-c}} \quad (5)$$

In this situation, referred to as the high pressure or fast energy exchange limit, the fraction of activated ions $[AB_{eq}^{+}*][AB^{+}]$ $(=k_c/k_{-c}$ from microscopic reversibility) reflects a Boltzmann distribution of internal energies. The situation is reversed in the low-pressure or slow energy exchange limit (i.e. the activation and deactivation rates are small relative to k_{uni}), so that the observed dissociation rate reflects the activation rate:

$$k_{diss} = k_c[M] \quad (6)$$

Unlike the rapid energy exchange situation, in which $[AB_{eq}^{+}*]$ is determined by the equilibrium established by activation/deactivation with a negligible contribution from dissociation, the slow energy exchange case gives rise to a steady-state concentration of the activated complex, $[AB_{ss}^{+}*]$. Figure 4 shows two hypothetical ion internal energy distributions illustrating the case in which dissociation is rate-limiting (rapid energy exchange) and the case in which the activation is rate-limiting (slow energy exchange).

A further consequence of the one-step activation process in Lindemann theory is that each collision of $[AB^{+}*]$ results in deactivation, an approximation termed the 'strong collision' assumption, so that $k_{-c}[M] = \omega$, where ω is the collision frequency. Then the equilibrium relaxation rate for activated ions is $\omega[AB_{eq}^{+}*]$ and the principle of detailed balancing requires that the activation rate at equilibrium or steady state is also $\omega[AB_{eq}^{+}*]$. Equating the steady-state rates of $[AB^{+}*]$ formation and loss then gives

$$\omega[AB_{eq}^{+}*] = (\omega + k_{uni})[AB_{ss}^{+}*] \quad (7)$$

Solving for $[AB_{ss}^{+}*]$ and recognizing that $d[A^{+}]dt = k_{uni}[AB_{ss}^{+}*] = k_{diss}[AB^{+}]$ gives the equation

$$k_{diss} = \frac{k_{uni}\,\omega}{\omega + k_{uni}}\frac{[AB_{eq}^{+}*]}{[AB^{+}]} = \int_{E_0}^{\infty}\frac{\omega}{\omega + k_{uni}}k_{uni}(E)P(E)\,dE \quad (8)$$

which is valid for the strong collision case at any energy exchange rate. $P(E)$ is the Boltzmann distribution function and k_{uni} is zero below E_0. Therefore, the observed (pressure-independent) rate constant at the fast energy exchange limit ($\omega \gg k_{uni}$) is the product of the unimolecular dissociation rate constant and the Boltzmann fraction of parent ions that are activated:

$$k_{diss} = k_{uni}\frac{[AB_{eq}^{+}*]}{[AB^{+}]} = \int_{E_0}^{\infty}k_{uni}(E)P(E)\,dE \quad (9)$$

Furthermore, at the slow (pressure-dependent) energy exchange limit ($k_{uni} \gg \omega$), the observed k_{diss} is determined by the product of collision frequency and the

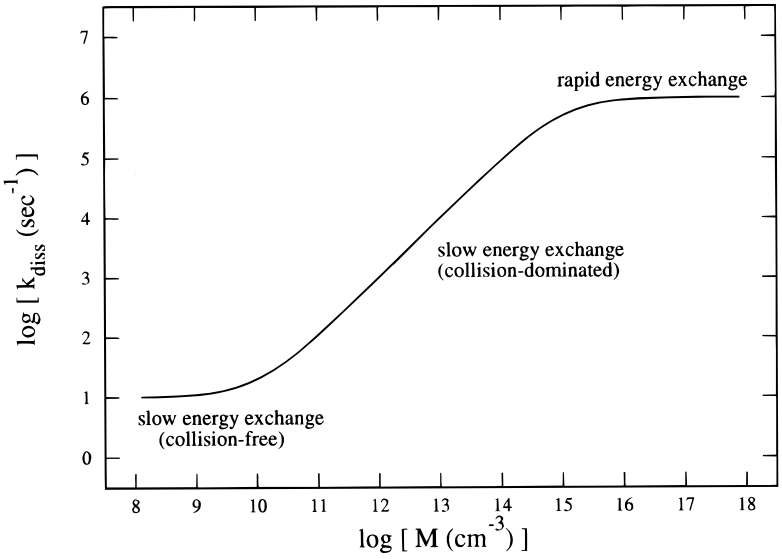

Figure 3. Log k_{diss} versus log[M] for a hypothetical ion with $k_{uni} = 10^6$ s^{-1}, k_c and $k_{-c} = 10^{-9}$ cm^3 molecule^{-1} s^{-1} and k_r and $k_{-r} = 10$ s^{-1}, as determined using Eqn (4).

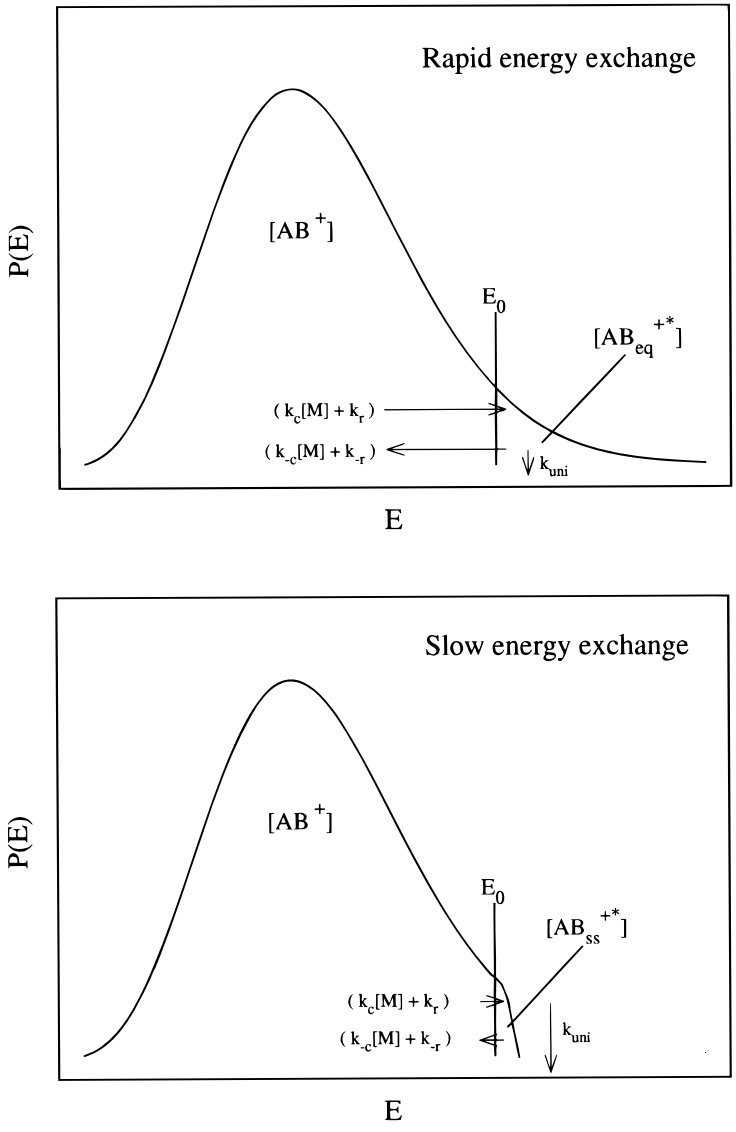

Figure 4. Hypothetical steady-state internal energy distributions for parent ions undergoing dissociation during the course of a slow heating activation process in (a) the rapid energy exchange limit and (b) the slow energy exchange limit. The lengths of the arrows indicate the relative magnitudes of the relevant rates. See text for definitions of the various symbols.

Boltzmann fraction of activated parent ions:

$$k_{\text{diss}} = \omega \int_{E_0}^{\infty} P(E)\, \mathrm{d}E \tag{10}$$

The k_{diss} of Eqn (9) is frequently referred to as the high-pressure first-order limit, whereas the k_{diss} of Eqn (10) is often referred to as the low-pressure second-order limit.

The above discussion of thermal unimolecular reactions at the high-and low-pressure limits for the strong collision case is useful in illustrating the roles of the relative rates of collisional activation, collisional deactivation and unimolecular dissociation in determining the observed fragmentation kinetics. However, the weak collision case is probably more applicable to the slow activation methods discussed in this review under most conditions. In such situations, excitation proceeds via small energy-exchange events (average energy-step size, ε), with up-steps ultimately being balanced by down-steps at the steady state. Thus, the collisional deactivation rate, $k_{-c}[\mathrm{M}] = \omega$, for strong collisions can be replaced by the corresponding expression for weak collisions at the steady state:[63]

$$k_{-c}[\mathrm{M}] = \omega \int_{E_0+\varepsilon}^{E_0} P(E)\, \mathrm{d}E P_{\text{down}}(E_0 + \varepsilon, E_0) = k_{\text{deact}} \tag{11}$$

where $P_{\text{down}}(E_0 + \varepsilon, E_0)$ is the probability that an energy down-step from within the interval $(E_0 + \varepsilon, E_0)$ will fall below E_0. Furthermore, at the steady state,

$$k_{\text{deact}} = k_{\text{act}} = \omega \int_{E_0-\varepsilon}^{E_0} P(E)\, \mathrm{d}E P_{\text{up}}(E_0 - \varepsilon, E_0) \tag{12}$$

where $P_{\text{u}}(E_0 - \varepsilon, E_0)$ is the probability that an up-step from within the interval $(E_0 - \varepsilon, E_0)$ will exceed E_0. Use

of the approach presented in the development of Eqn (8) leads to the following expression for k_{diss} in the weak collision case at any energy exchange rate:

$$k_{diss} = \frac{k_{act}}{k_{uni} + k_{act}} \int_{E_0}^{\infty} k_{uni}(E)P(E)\,dE \qquad (13)$$

At the fast energy exchange limit ($k_{act} \gg k_{uni}$), Eqn (13) reduces to the same expression as given for k_{diss} in the strong collision case (Eqn (9)). However, the slow energy exchange limit for k_{diss} differs from that obtained in the strong collision situation (Eqn (10)) by the second integral in Eqn (14), which is less than unity:

$$k_{diss} = \omega \int_{E_0}^{\infty} P(E)\,dE \int_{E_0-\varepsilon}^{E_0} P(E)\,dE P_{up}(E_0 - \varepsilon, E_0) \qquad (14)$$

Whether the slow heating method is performed under conditions of rapid or slow energy exchange has important implications with respect to the relationship between the experimentally observed dissociation rate, k_{diss}, and fundamental properties of the ion, such as the dissociation threshold. In the case of the rapid energy exchange limit, the situation is straightforward in that k_{diss} is determined by the unimolecular dissociation rate, k_{uni}, of a population of ions with a Boltzmann distribution of internal energies (see Eqn (9)). A plot of ln k_{diss} versus 1/T yields the true Arrhenius activation energy (via the slope) and pre-exponential factor (intercept). Provided conditions of rapid energy exchange are established, all methods of activation yield the same result. The situation is much more complex, however, in the slow energy exchange regime. In this case, k_{diss} reflects characteristics of the activation method as well as the dissociation threshold (through the integral expressions in Eqn (10) or (14)). Determination of the quantitative relationship between k_{diss} and the dissociation threshold, therefore, requires modeling of the activation process.

The appearance of the tandem mass spectrum may also be affected by the activation method depending upon which energy transfer regime, fast versus slow, applies. In the rapid energy transfer case, the internal energy distribution of the parent ions that yield first-generation product ions is defined by the Boltzmann equation and is therefore independent of the nature of the activation method. On the other hand, in the slow energy transfer regime, differences in the magnitudes and distributions of the energy step sizes associated with the various activation methods could result in differences in the internal energy distributions of the fragmenting ions. Such a difference, in turn, could lead to differences in the identities and relative abundances of the first-generation product ions in tandem mass spectra obtained using different activation methods, despite the fact that the energy distributions of the non-fragmenting parent ions are very similar. In either the fast or slow energy exchange regime, the appearance of the tandem mass spectrum can also be significantly affected by the conditions applied to the product ions. In some cases, for example, first-generation product ions are not subjected to further activation whereas in other cases, product ions can themselves undergo further activation.

SLOW HEATING METHODS IN TANDEM MASS SPECTROMETRY

This discussion is focused on activation methods that employ activation periods of $\sim 10^{-2}$ s or greater. The criterion used here to distinguish a 'slow heating' method from other forms of activation is that a condition is reached in which the rates for activation and deactivation are equal, yielding a steady-state parent ion internal energy distribution. While such a condition can be achieved in less than 10^{-2} s, activation periods in ion trapping instruments are at least this long to allow for efficient conversion of parent ions to product ions. The activation period itself is chosen to be consistent with k_{diss} which, in turn depends upon either the activation rate (slow energy exchange, Eqn (10) or (14)) or the unimolecular dissociation rate (rapid energy exchange, Eqn (9)). The variation in activation periods among the slow heating methods (see Figure 1) is largely due to differences in activation conditions that lead to differences in k_{diss}.

The major slow heating methods involve heating and cooling via collisions, photon absorption/emission or both. For the collision-dominated methods in ion trapping instruments, the commonly employed tactic is to accelerate the ions in a more or less continuous fashion in the presence of background atoms or molecules. An upper limit to the achievable $T_{internal}$ is imposed by parent ion ejection from the trap. That is, the upper limit to kinetic energy for ion storage leads to an upper limit to the achievable $T_{internal}$. The collisionless methods, on the other hand, do not involve parent ion acceleration. Furthermore, the collision methods usually involve parent ion acceleration that is mass-to-charge ratio dependent such that product ions once formed are not subjected to ion acceleration. The collisionless methods, however, typically yield product ions that can undergo further activation under essentially the same conditions as the parent ions. Therefore, the extent to which products from sequential ion decomposition appear in tandem mass spectra derived using the various slow heating methods can differ, as mentioned above. The major slow heating methods so far employed within the context of a tandem mass spectrometric experiment are briefly discussed below.

Infrared multiphoton dissociation using low power cw lasers

Infrared multiphoton dissociation (IRMPD) has been effected both with high-power pulsed lasers (MW cm^{-2})[57–59] and with relatively low <100 W cm^{-2}) continuous-wave (cw) lasers using irradiation times of tens to hundreds of milliseconds.[13–16,20,64–80] The latter approach constitutes a slow heating method and has been implemented primarily in ion cyclotron resonance[13–16,20,64–73] and quadrupole ion trap[74–80] instruments. The major distinction between the two approaches to IRMPD arises from the importance of spontaneous IR emission from the ion during the activation process. In the case of high-power pulsed

IRMPD, spontaneous IR emission during the laser pulse is negligible, thereby making the dissociation yield dependent solely on laser fluence and not on laser intensity (at constant fluence). Dissociation yields using low-power cw IRMPD, on the other hand, are highly dependent upon the laser intensity at constant fluence. Much of the work using low-power cw IRMPD to date has emphasized the tendency of the technique to promote the lowest energy decomposition reaction.

Applications have been largely focused on ion chemistry issues of modest sized polyatomic ions. Recently, however, Little et al.[73] have reported the use of low-power IRMPD for multiply charged biomolecules of mass in the tens of kilodaltons in an ion cyclotron resonance instrument. A number of attractive features of this approach were noted including the rich structural information that resulted, which contrasted with the formation of small uninformative fragments resulting from the use of UV photodissociation.[81] In contrast with collisional activation methods, which require the use of higher background pressures and acceleration of the ion population, photodissociation leads to minimal perturbation of ion motion in the ion cyclotron resonance cell with consequent advantages in mass measurement. Stephenson et al.[79] have also recently demonstrated slow IRMPD of biologically relevant ions in a quadrupole trap. It seems likely, therefore, that cw IRMPD may see increasing application as an activation method for structural studies of bio-ions.

Dunbar and co-workers[60,70–72]have modeled the cw IRMPD process to explore the possibility of deriving fundamental information, such as thresholds for dissociation, from the experimentally derived dissociation rate. Much of this modeling effort has direct relevance to other slow activation methods and provides insights into various phenomena, such as photon absorption, emission, dissociation and collisions, that can take place during the activation period. In general terms, Dunbar and co-workers showed that an ion population exposed to low-power IR irradiation achieves a Boltzmann distribution of internal energies, which can be specified in terms of an internal temperature that is directly related to laser intensity. The kinetics of dissociation can therefore be treated on the basis of Boltzmann statistics, with some adjustments arising from the effect of dissociation on the shape of the internal energy distribution, resulting from the fact that the slow energy exchange condition applies to the modeled ions. An Arrhenius activation energy is derived from the experimentally derived rate, which, in turn, is related to the critical energy for dissociation via a modified form of the Tolman theorem.[60]

In modeling cw IRMPD, it is assumed that the dissociation kinetics do not reflect a rate-limiting passage through an energy bottleneck in the laser up-pumping process. Rather, for ions in the slow energy exchange regime, dissociation kinetics are determined by the laser up-pumping processes near dissociation threshold. Moderately large polyatomic ions at room temperature are generally characterized by vibrational state densities in excess of the bandwidth of a typical IR laser and are therefore considered to be in the quasi-continuum of vibrational states thereby making the above assumption a reasonable one.

Dissociation by blackbody radiation

It has recently been demonstrated that ion activation via absorption of blackbody radiation under essentially collision-free conditions can lead to ion dissociation.[21,82–89] The high vacuum environment of the ion cyclotron resonance instrument and its ability to allow for long storage times have allowed for the clear demonstration that the dissociation rate does not extrapolate to zero at zero pressure for some ions, thereby implicating dissociation driven by photodissociation. Dunbar[84] recognized the close similarity between this phenomenon and the cw IRMPD experiment and described the kinetics for blackbody radiation-driven dissociation in the same terms used for cw IRMPD. Indeed, the blackbody case is the simplest to model and therefore promises to be an effective means for the study of thermochemical aspects of ion dissociation.

Williams' group has examined the blackbody radiation-driven dissociation of a variety of ions derived from biopolymers[87–89] with attention paid both to analytical aspects of the phenomenon and to the dissociation kinetics for high mass ions. They have shown, for example, that ions derived from bovine ubiquitin can be dissociated with essentially 100% efficiency at 200 °C over a period of 20 s. It was also pointed out that blackbody-driven dissociation enjoys many of the advantages of cw IRMPD but requires no laser. As with the other very slow activation methods, however, dissociation reactions requiring the least energy tend to dominate the spectrum. Furthermore, particularly stable ions, an example was shown to be triply protonated melittin,[87] may require temperatures in excess of 200 °C to observe fragmentation.

An interesting consequence of the large number of degrees of freedom of high-mass bio-ions is that the kinetics of dissociation driven by blackbody radiation yield the "high-pressure' limit or rapid energy exchange result despite the fact that the ions undergo an insignificant number of collisions.[89] That is, the rate of energy exchange by photon absorption and emission is rapid relative to the dissociation rate of the excited ion (k_r, $k_{-r} \gg k_{uni}$) so that k_{diss} is given by Eqn (9). Strong evidence was presented by Price *et al.*[89] that ions derived from bovine ubiquitin underwent dissociation at pressure-independent rates, consistent with those expected for the rapid energy exchange limit despite the fact that collision rates were far too low to give rise to this condition. This study is the first to demonstrate achievement of the rapid energy exchange condition within the context of a tandem mass spectrometric experiment. The dissociation rate can therefore be used to obtain the true Arrhenius activation energies and A-factors directly, providing a highly useful tool for the study of bio-ion dissociation.

Quadrupole ion trap collisional activation

Collisional activation in the quadrupole ion trap was first demonstrated using parent ion acceleration via resonance excitation with relatively low (<1 V zero-to-peak) resonance excitation voltages and activation times

of less than 100 ms.[17] In fact, ion activation times as short as 10 ms can yield a sufficient number of collisions to produce high dissociation efficiencies.[17,90,91] These activation times are relatively short for a slow heating method and primarily reflect the relatively high collision rates resulting from the use of helium as a background gas at roughly 1 mTorr (1 Torr = 133.3 Pa). While a variety of other approaches to parent ion acceleration for the purpose of collisional activation in the ion trap have been described,[92–96] the single frequency resonance excitation approach is emphasized here because of its wide usage and the fact that ion dissociation energies have been empirically correlated with resonance excitation voltages required to achieve a fixed value of k_{diss}.[97,98] Such behavior is expected for ions that achieve the steady-state internal energy condition, which results from the use of a continuous ion acceleration method (see below).

A mathematical model and related random walk simulation for the collisional activation process have been developed using the kinetic theory of ion transport in gases, the forced damped harmonic oscillator model for resonance excitation and thermal activation theory.[99,63] Although this model does not account for complexities introduced into the parent ion acceleration process associated with non-linear ion traps,[100,101] it demonstrates qualitatively the evolution of events in the collisional activation process. The overall thermal picture applies for any continuous ion acceleration method. Figure 5 shows the results of a random walk simulation of the ion internal energy distribution of a population of n-butylbenzene molecular ions (dissociation neglected) subjected to on-resonance excitation (215 mV) for 57 ms (10^4 ion–helium collisions) in the presence of room temperature helium at 1 mTorr. Regardless of the assumed initial parent ion internal energy distribution, the final steady-state distribution in shown in the figure. The points show the results of the simulation and the curve is a calculated Boltzmann distribution for $T_{internal} = 500$ K. In analogy with Dunbar's work in modeling cw IRMPD, in which it was shown that low-intensity cw irradiation of an ion population at a fixed frequency leads to a Boltzmann distribution of internal energies (for a non-fragmenting ion population),[60] single-frequency resonance excitation in the quadrupole ion trap also leads to a Boltzmann distribution of parent ion internal energies at the steady state. The simulation of Figure 5 was allowed to run for tens of milliseconds. However, the model suggests that the steady-state condition is reached relatively early in the resonance excitation process.

Figure 6 shows a calculated Boltzmann distribution of internal energies for *n*-butylbenzene at 300 K and results of a random walk simulation using the conditions leading to the result of Figure 5 for 10 collisions (diamonds) and 100 collisions (filled circles). It is apparent that significant changes in the internal energy distribution occur for just 10 ion–helium collisions. By the time 100 collisions have occurred (<1 ms of resonance excitation), the steady-state condition has been reached (i.e. a Boltzmann distribution for $T_{internal} = 500$ K has been achieved). No further changes in the distribution are observed as more collisions occur. The steady-state condition is reached quickly relative to typical values of k_{diss}, indicating that, under common experimental conditions, parent ions can achieve the steady-state condition before extensive dissociation occurs and that k_{diss} might be modeled based on either the rapid energy or slow energy exchange conditions. The observed k_{diss} for *n*-butylbenzene ions has been modeled using the assumption of parent ion 'sudden death', which corresponds to the slow energy exchange condition and weak collisions yielding results qualitatively consistent with experiment.[63] While quantitative reproduction of the experimental results would probably be fortuitous at this stage in the development of the model, given uncertainties in the collisional energy transfer parameters in the model, uncertainty in the dissociation threshold for the ion and the simplistic assumption of harmonic parent ion motion in a pure quadrupole field, it shows

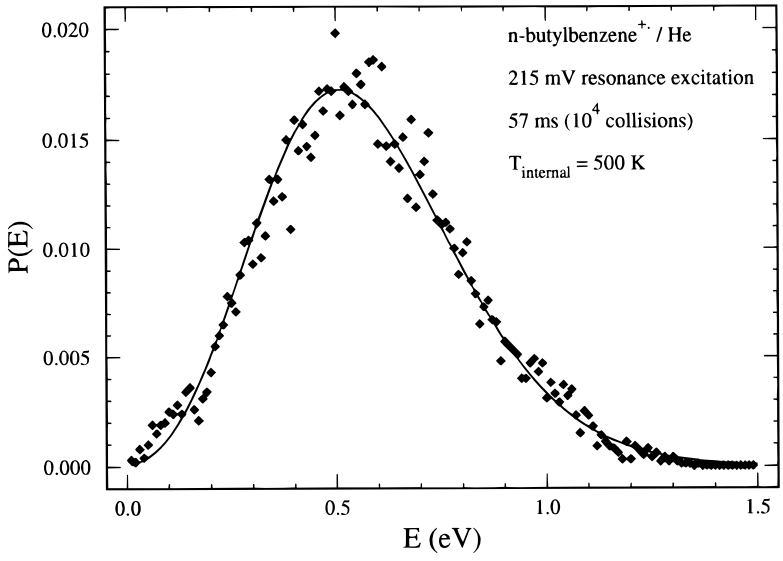

Figure 5. Results of a random walk simulation of the ion internal energy distribution of a population of *n*-butylbenzene molecular ions (dissociation neglected) subjected to on-resonance excitation (215 mV) for 57 ms (10^4 ion–helium collisions) in the presence of room temperature helium at 1 mTorr.

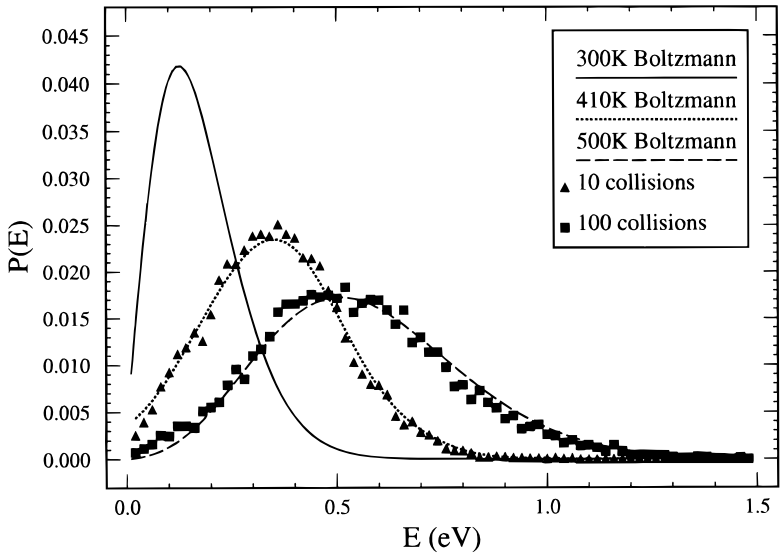

Figure 6. Calculated Boltzmann distribution of internal energies for *n*-butylbenzene ions at 300 K (solid line) and results of a random walk simulation using the conditions leading to the result of Fig. 5 for 10 collisions (diamonds) and 100 collisions (filled circles).

the experimentally observed induction period and exponential parent ion loss.

Ion cyclotron resonance collisional activation

To deposit relatively large amounts of internal energy per collision and to minimize ejection for precursor ions, conventional collisional activation in ICR-MS is achieved with a short duration (hundreds of μs), relatively high-amplitude (hundreds of volts) radiofrequency excitation pulse at the resonant frequency of the precursor ion.[102–104] Two variations of the on-resonance excitation method have been developed to allow for slow heating without increasing ion losses due to ejection: sustained off-resonance irradiation (SORI)[18] and very low energy collisional activation (VLE-CA).[105,106] Both approaches involve a more or less continuous process of parent ion acceleration and deceleration and are therefore expected to give rise to a steady-state internal energy distribution, at least under some conditions. A related technique, multiple excitation collisional activation (MECA),[107] can also enhance the dissociation efficiency by repeated excitation of any intact parent ions which have returned to the center of the ion cell due to kinetic energy-dissipating ion–neutral collisions. The overall duration of a sequence of many such excitation–relaxation cycles may extend into the time regime associated with very slow activation methods. However, conventional pulsed resonant excitation is used for each individual activation event so that a steady-state condition of energy up- and down-steps may not be reached. All of these modified methods share the characteristics of increased resolving power in the second stage of mass spectrometry (owing to minimal ion cloud distortion and the associated longer lasting transients) and minimal secondary fragmentation.

In the SORI technique, a signal shifted away from the resonant frequency is used for ion excitation, so that ions undergo many acceleration–deceleration cycles during the excitation period.[108] Because the ion translational energy is small compared with on-resonance excitation, much longer ion activation times can be achieved without significant ion ejection. Using a non-resonant frequency corresponding to an m/z value greater than a (singly charged) precursor ion avoids ejection or excitation of product ions, i.e. blind spots. However, two separate experiments at different excitation frequencies are required for multiply charged precursor ions because product ions appear at m/z values on either side of the precursor.[109] SORI has been shown to be effective in dissociating both relatively small ions[17] and larger ions derived from peptides[110] and proteins.[109] Marzluff and Beauchamp[111] pointed out that the SORI process is amenable to modeling via a master equation analysis, just as cw IRMPD, ion trap collisional activation and dissociation driven by blackbody radiation are and gave a preliminary report of application to SORI.

Very low energy collisional activation

As in SORI, the kinetic energy of precursor ions is moderated by multiple acceleration–deceleration cycles, albeit by repeated phase inversion of the resonant excitation signal.[112] High-resolution control of the kinetic energy is achieved by adjustment of the signal amplitude and delay between 180° phase shifts.[105,106] However, blind spots can also appear with this method because rapid phase inversion produces a frequency-domain excitation spectrum having a Lorentzian-like envelope of evenly spaced spikes centered at the resonance frequency. A variation of the VLE-CA method, referred to as RAM-CAD,[109] limits the number of spikes to two by amplitude modulation of the unshifted resonance excitation signal.

Although there are differences in how parent ion acceleration is effected, the dynamics of SORI and VLE-CA appear to be very similar and the two

methods yield similar results. VLE-CA should also be amenable to modeling in analogy with the other slow heating methods, but no reports on this topic have appeared.

FIGURES OF MERIT OF SLOW HEATING METHODS

While the reader is encouraged to consider the figures of merit for each specific very slow activation method, they are considered here collectively to contrast them with the faster activation methods. Specifically, we consider the limiting case in which the ion population reaches a steady-state Boltzmann (rapid energy exchange limit) or near-Boltzmann (slow energy exchange regime with a relatively small part of the high energy tail exceeding the dissociation threshold) distribution of internal energies.

The amount of energy that can be deposited into the ion via a very slow activation method is determined by the maximum temperature to which the ions can be elevated. This may be determined by the temperature of the walls, laser intensity, maximum ion oscillatory amplitude, etc., depending on the activation method. It is important to recognize, in any case, that a major strength of very slow activation methods has been that they have been shown to be capable of yielding useful structural information from high-mass ions.[73,79,87,89,109,110,113] The limitations for conventional collisional activation of high-mass ions with many degrees of freedom arising from unfavorable center-of-mass collision energy and high ion heat capacity is circumvented by the slow heating nature of the very slow activation methods. Any polyatomic ion can be made to dissociate if the temperature is high enough.

In the limiting case, the shape of the ion internal energy distribution for an ion population with fragmentation taking place in the high-energy tail is a truncated Boltzmann distribution when fragmentation is fast relative to activation/deactivation, and Boltzmann when fragmentation is slow relative to activation/deactivation. Although the internal energy distribution is broad, it is very well known, at least for the rapid energy exchange case. Such a situation is desirable for the determination of dissociation energies, for example.

The parent ion internal temperature is readily variable with the collisional activation techniques via either resonance excitation amplitude or frequency. Laser intensity is the most readily varied parameter related to ion temperature in cw IRMPD. In the case of blackbody activation, the temperature of the walls of the ion containment vessel must be varied.

A great strength of the very slow activation methods is that dissociation reactions can be driven to essentially 100% completion under favorable conditions. This ability arises from variable storage time and variable ion temperatures. In the case of dissociation, the parent ion temperature must be elevated to a point at which the high energy tail of the distribution exceeds the lowest critical energy for decomposition enough to make the dissociation rate sufficiently high to yield products during the activation time. Once this condition is achieved, the activation period can be extended to allow for all of the parent ions to dissociate. In practice, and depending upon the activation method, it may not be desirable to do this due to further activation of the products, ion–neutral reactions, etc. While dissociation efficiency is high, the identities of the product ions tend to be restricted to those generated from the reactions of lowest critical energy. The degree to which these products provide the desired structural information is case dependent.

In some scenarios, the length of the activation period associated with a very slow activation method may constitute a serious weakness. That is, the time required for efficient conversion of parent ions to product ions may not be appropriate for some analytical applications. For example, the many seconds required for some blackbody activated reactions would be incompatible with many MS/MS experiments coupled with on-line separations. On the other hand, activation periods of a few tens to a few hundreds of milliseconds may constitute only a minor fraction of the total time associated with a trapped ion MS/MS experiment. That is, other aspects of trapped ion experiments are also time consuming compared with, for example, beam-type or time-of-flight mass spectrometry.

CONCLUSIONS

Several approaches to the activation of polyatomic ions over extended periods of time have been developed principally in conjunction with ion trapping forms of mass spectrometry. Conditions can be achieved in which the rates for ion activation and deactivation are comparable, resulting in a steady-state parent ion internal energy distribution. Under these conditions, a thermal analogy can be used to interpret the observed k_{diss}. The relationship between k_{diss} and the dissociation threshold of the ion depends on the rates of energy exchange relative to unimolecular dissociation rates. Furthermore, the appearance of the product ion spectrum can also depend on whether fast or slow energy exchange conditions apply and on whether product ions are subjected to the same activation conditions as the parent ions.

It is important to recognize that the thermal analogy is a useful limiting case in considering slow heating methods. There are a variety of scenarios in which conditions that lead to a near-Boltzmann distribution of ion internal energies do not prevail. For example, when the critical energy for dissociation is not particularly high relative to the average internal energy of the ion population, a truncated Boltzmann distribution is not realistic. Likewise, when dissociation proceeds at a significant rate before a steady-state condition is achieved, recourse to the master equation modeling approach is required for calculating the dissociation rate constant.

As with all forms of ion activation, the analytical figures of merit of slow heating methods are better suited to some applications than to others. The use of slow heating methods, however, is expected to grow

owing both to the growing numbers of ion trapping instruments in operation and to the success of slow heating in the efficient dissociation ions derived from high-mass biomolecules. In addition to offering high efficiency, an MS/MS experiment using a slow heating method can yield important information about an ion both from the identities and relative abundances of the product ions and from k_{diss}. Furthermore, a detailed understanding of the relationship between $T_{internal}$, k_{diss} and dissociation threshold promises to yield an important new tool in understanding the unimolecular dissociation chemistry of high-mass ions.

Acknowledgements

Dr James L. Stephenson, Jr, is acknowledged for helpful discussions. This work was sponsored by the Office of Basic Energy Sciences, US Department of Energy, under Contract DE-AC05–96OR22464 with Oak Ridge National Laboratory, managed by Lockheed Martin Energy Research Corp.

REFERENCES

1. J. R. Chapman, *Practical Organic Mass Spectrometry*. Wiley, Chichester (1985).
2. B. J. Millard, *Quantitative Mass Spectrometry*. Heyden, London (1979).
3. F. W. McLafferty (Ed.), *Tandem Mass Spectrometry*. Wiley, New York (1983).
4. K. L. Busch, G. L. Glish and S. A. McLuckey, *Mass Spectrometry/Mass Spectrometry: Techniques and Applications of Tandem Mass Spectrometry*. VCH, New York (1988).
5. S. E. Kupriyanov and A. A. Perov, *Russ. J. Phys. Chem.* 39, 871 (1965).
6. K. R. Jennings, *Int. J. Mass Spectrom. Ion Phys.* **1**, 227 (1968).
7. W. F. Haddon and F. W. McLafferty, *J. Am. Chem. Soc.* **90**, 4745 (1968).
8. R. A. Yost and C. G. Enke, *J. Am. Chem. Soc.* **100**, 2274 (1978).
9. R. A. Yost and C. G. Enke, *Anal. Chem.* **51**, 1251A (1979).
10. R. B. Cody and B. S. Freiser, *Int. J. Mass Spectrom.* Ion Phys. **41**, 199 (1982).
11. R. G. Cooks, T. Ast and Md. A. Mabud, *Int. J. Mass Spectrom. Ion Processes* **100**, 209 (1990).
12. R. B. Cody and B. S. Freiser, *Anal. Chem.* **51**, 547 (1979).
13. R. C. Dunbar, in *Gas Phase Ion Chemistry*, edited by M. T. Bowers, Vol. 2, Chapt. 14. Academic Press, New York (1979).
14. R. C. Dunbar, in *Gas Phase Ion Chemistry*, edited by M. T. Bowers, Vol. 3, Chapt. 20. Academic Press, New York (1984).
15. L. R. Thorne and J. L. Beauchamp, in *Gas Phase Ion Chemistry*, edited by by M. T. Bowers, Vol. 3, Chapt. 18. Academic Press, New York (1984).
16. R. C. Dunbar, in *Molecular Ions: Spectroscopy, Structure and Chemistry*, edited by T. A. Miller. North-Holland, Amsterdam (1983).
17. R. Orlando, C. Fenselau and R. J. Cotter, *J. Am. Soc. Mass Spectrom.* **2**, 189 (1991).
18. J. W. Gauthier, T. R. Trautman and D. B. Jacobson, *Anal. Chim. Acta* **246**, 211 (1991).
19. J. N. Louris, R. G. Cooks, J. E. P. Syka, P. E. Kelley, G. C. Stafford, Jr, and J. F. J. Todd, *Anal. Chem.* **59**, 1677 (1987).
20. R. L. Woodin, R. S. Bomse and J. L. Beauchamp, *J. Am. Chem. Soc.* **100**, 3248 (1978).
21. D. Thölmann, D. S. Tonner and T. B. McMahon, *J. Phys. Chem.* **98**, 2002 (1994).
22. K. Vékey, *J. Mass Spectrom.* **31**, 445 (1996).
23. M. S. Kim and F. W. McLafferty, *J. Am. Chem. Soc.* **100**, 3279 (1978). 24. S. A. McLuckey, G. L. Glish and R. G. Cooks, *Int J. Mass Spectrom. Ion Phys.* **39**, 219 (1982).
25. C. Lifshitz, *J. Phys. Chem.* **87**, 2304 (1983).
26. J. C. Lorquet, *Mass Spectrom. Rev.* **13**, 233 (1994).
27. W. Forst, *Theory of Unimolecular Reactions*. Academic Press, New York (1973).
28. P. J. Robinson and K. A. Holbrook, *Unimolecular Reactions*. Wiley, Chichester (1972).
29. A. K. Shukla, K. Qian, S. G. Anderson and J. H. Futrell, *J. Am. Soc. Mass Spectrom.* **1**, 6 (1990).
30. P. J. Todd and F. W. McLafferty, *Int. J. Mass Spectrom Ion Phys.* **38**, 371 (1981).
31. D. J. Douglas, *J. Phys. Chem.* **86**, 185 (1982).
32. M. S. Kim, *Int. J. Mass Spectrom. Ion Phys.* **50**, 189 (1983).
33. M. S. Kim, *Int. J. Mass Spectrom. Ion Phys.* **51**, 279 (1983).
34. C. E. D. Ouwerkerk, S. A. McLuckey, P. G. Kistemaker and A. J. H. Boerboom, *Int. J. Mass Spectrom Ion Processes* **56**, 11 (1984).
35. R. K. Boyd, Int. *J. Mass Spectrom. Ion Processes* **75**, 243 (1987).
36. K. L. Schey, H. I. Kenttämaa, V. H. Wysocki and R. G. Cooks, *Int. J. Mass Spectrom. Ion Processes* **90**, 71 (1989).
37. M. L. Gross, K. B. Tomer, R. L. Cerny and D. E. Giblin, in *Mass Spectrometry in the Analysis of Large Molecules*, edited by C. J. McNeal. Wiley, New York, 1986.
38. R. D. Smith, J. A. Loo, C. G. Edmonds, C. J. Barinaga and H. R. Udseth, *Anal. Chem.* **62**, 882 (1990).
39. M. Busman, A. L. Rockwood and R. D. Smith, *J. Phys. Chem.* **96**, 2397 (1992).
40. M. Meot-Ner, A. R. Dongré, A. Somogyi and V. H. Wysocki, *Rapid Commun. Mass Spectrom.* **9**, 829 (1995).
41. W. J. van der Hart, *Int. J. Mass Spectrom. Ion Processes* **118/119**, 617 (1992).
42. R. E. Tecklenberg, Jr, and D. H. Russell, *Mass Spectrom. Rev.* **9**, 405 (1990).
43. W. J. van der Hart, *Mass Spectrom. Rev.* **8**, 237 (1989).
44. F. M. Harris and J. H. Beynon, in *Gas Phase Ion Chemistry*, edited by M. T. Bowers, Vol. 3, Chapt. 19. Academic Press, New York (1984).
45. J. Durup, in *Recent Developments in Mass Spectrometry*, edited by K. Ogata and T. Hayakawa, p. 921. University Park Press, Baltimore (1970).
46. K. Levsen and H. Schwartz, *Mass Spectrom. Rev.* **2**, 77 (1983).
47. P. J. Todd and F. W. McLafferty, in *Tandem Mass Spectrometry*, edited by F. W. McLafferty, p. 149. Wiley, New York (1983).
48. P. H. Dawson and D. J. Douglas, in *Tandem Mass Spectrometry*, edited by F. W. McLafferty, p. 125. Wiley, New York (1983).
49. S. Singh, F. W. Harris, R. K. Boyd and J. H. Beynon, *Int. J. Mass Spectrom Ion Processes* **66**, 131 (1985).
50. R. N. Hayes and M. L. Gross, In *Methods in Enzymology*, Vol. 19: Mass Spectrometry, edited by J. A. McCloskey, Chapt. 10. Academic Press, Orlando (1990).
51. M. S. Kim, *Org. Mass Spectrom.* **26**, 565 (1991).
52. S. A. McLuckey, *J. Am. Soc. Mass Spectrom.* **3**, 599 (1992).
53. A. K. Shukla and J. H. Futrell, *Mass Spectrom. Rev.* **12**, 211 (1993).
54. R. G. Cooks, *J. Mass Spectrom.* **30**, 1215 (1995).
55 R. G. Cooks, T. Ast, T. Pradeep and V. H. Wysocki, *Acc. Chem. Res.* **27**, 316 (1994).
56. A. R. Dongré, A. Somogyi and V. H. Wysocki, *J. Mass Spectrom.* **31**, 339 (1996).
57. R. N. Rosenfeld, J. M. Jasinski and J. I. Brauman, *J. Am. Chem. Soc.* **101**, 3999 (1979).
58. M. Quack, *Infrared Phys.* **29**, 441 (1989).
59. D. Lupo and M. Quack, *Chem. Rev.* **87**, 181 (1987).
60. R. C. Dunbar, *J. Chem. Phys.* **95**, 2537 (1991).
61. F. A. Lindemann, *Trans. Faraday Soc.* **17**, 598 (1922).
62. R. E. Westin, Jr, and H. A. Schwarz, *Chemical Kinetics*. Prentice-Hall, Englewood Cliffs, NJ (1972).
63. D. E. Goeringer and S. A. McLuckey, *Rapid Commun. Mass Spectrom.* **10**, 328 (1996).

64. J. M. Jasinski, R. N. Rosenfeld, F. K. Meyer and J. I. Brauman, *J. Am. Chem. Soc.* **104**, 652 (1982).
65. W. Tumas, R. F. Foster, M. J. Pellerite and J. I. Brauman, *J. Am. Chem. Soc.* **105**, 7464 (1983).
66. W. Tumas, R. F. Foster and J. I. Brauman, *Isr. J. Chem.* **24**, 223 (1984).
67. C. H. Watson, G. Baykut and J. R. Eyler, *Anal. Chem.* **59**, 1133 (1987).
68. M. Moini and J. R. Eyler, *Int. J. Mass Spectrom. Ion Processes* **76**, 47 (1987).
69. M. Bensimon, J. Rapin and T. Gaumann, *Int. J. Mass Spectrom. Ion Processes* **72**, 125 (1986).
70. G. T. Ueci and R. C. Dunbar, *J. Chem. Phys.* **96**, 8897 (1992).
71. R. C. Dunbar and R. C. Zaniewski, *J. Chem. Phys.* **96**, 5069 (1992).
72. G. T. Uechi and R. C. Dunbar, *J. Chem. Phys.* **98**, 7888 (1993).
73. D. P. Little, J. P. Speir, M. W. Senko, P. B. O'Connor and F. W. McLafferty, *Anal. Chem.* **66**, 2809 (1994).
74. R. J. Hughes, R. E. March and A. B. Young, *Int. J. Mass Spectrom. Ion Phys.* **42**, 255 (1982).
75. R. J. Hughes, R. E. March and A. B. Young, *Can. J. Chem.* **61**, 834 (1983).
76. R. J. Hughes, R. E. March and A. B. Young, *Int. J. Mass Spectrom. Ion Phys.* **47**, 85 (1983).
77. R. J. Hughes, R. E. March and A. B. Young, *Can. J. Chem.* **63**, 2324 (1985).
78. J. L. Stephenson, Jr, M. M. Booth, J. A. Shalosky, J. R. Eyler and R. A. Yost, *J. Am. Soc. Mass Spectrom.* **5**, 886 (1994).
79. J. L. Stephenson, Jr, M. M. Booth, S. M. Boue, J. R. Eyler and R. A. Yost, in *Biochemical and Biotechnical Applications of Electrospray Ionization Mass Spectrometry*, edited by A. P. Snyder, p. 512. Academic Press, San Diego (1996).
80. A. Colorado, J. X. Shen; V. H. Vartanian and J. Brodbelt, *Anal. Chem.* **68**, 4033 (1996).
81. S. C. Beu, M. W. Senko, J. P. Quinn, F. M. Wampler, III, and F. W. McLafferty, *J. Am. Soc. Mass Spectrom.* **4**, 557 (1993).
82. M. Sena and J. Riveros, *Rapid Commun. Mass Spectrom.* **8**, 1031 (1994).
83. D. S. Tonner, D. Thölmann and T. B. McMahon, *Chem. Phys. Lett.* **233**, 324 (1995).
84. R. C. Dunbar, *J. Phys. Chem.* **98**, 8705 (1994).
85. R. C. Dunbar, T. B. McMahon, D. Thölmann, D. S. Tonner, D. R. Salahub and D. Wei, J. *Am. Chem. Soc.* **117**, 12819 (1995).
86. C. Y. Lin and R. C. Dunbar, *J. Phys. Chem.* **100**, 655 (1996).
87. W. D. Price, P. D. Schnier and E. R. Williams, *Anal. Chem.* **68**, 859 (1996).
88. P. D. Schnier, W. D. Price, R. A. Jockusch and E. R. Williams, *J. Am. Chem. Soc.* **118**, 7178 (1996).
89. W. D. Price, P. D. Schnier, R. A. Jockusch, E. F. Strittmatter and E. R. Williams, *J. Am. Chem. Soc.* **118**, 10640 (1996).
90. J. Gronowska, C. Paradisi, P. Traldi and U. Vettori, *Rapid Commun. Mass Spectrom.* **4**, 306 (1990).
91. M. J. Charles, S. A. McLuckey and G. L. Glish, *J. Am. Soc. Mass Spectrom.* **5**, 1031 (1994).
92. S. A. McLuckey, D. E. Goeringer and G. L. Glish, *Anal. Chem.* **64**, 1455 (1992).
93. S. A. Lammert and R. G. Cooks, *Rapid Commun. Mass Spectrom.* **6**, 528 (1992).
94. C. Paradisi, J. F. J. Todd and U. Vettori, *Org. Mass Spectrom.* **27**, 251 (1992).
95. M. Wang, S. Schachterle and G. Wells, *J. Am. Soc. Mass Spectrom.* **7**, 668 (1996).
96. J. Qin and B. T. Chait, *Anal. Chem.* **68**, 2108 (1996).
97. K. J. Hart and S. A. McLuckey, *J. Am. Soc. Mass Spectrom.* **5**, 250 (1994).
98. A. Colorado and J. Brodbelt, *J. Am. Soc. Mass Spectrom.* **7**, 1116 (1996).
99. D. E. Goeringer and S. A. McLuckey, *J. Chem. Phys.* **104**, 2214 (1996).
100. J. Franzen, R.-H. Gabling, M. Schubert and Y. Wang, in *Practical Aspects of Ion Trap Mass Spectrometry*, edited by R. E. March and J. F. J. Todd, Vol. 1, p. 49. CRC Press, Boca Raton, FL (1995).
101. M. Splendore, F. A. Londry, R. E. March, R. J. S. Morrison, P. Perrier and J. André, *Int. J. Mass Spectrom. Ion Processes* **156**, 11 (1996).
102. R. B. Cody, R. C. Burnier and B. S. Freiser, *Anal. Chem.* **54**, 96 (1982).
103. T. J. Carlin and B. S. Freiser, Anal. Chem. **55**, 571 (1983).
104. R. C. Burnier, R. B. Cody and B. S. Freiser, *J. Am. Chem. Soc.* **104**, 7436 (1982).
105. K. A. Boering, J. Rolfe and J. I. Brauman, *Rapid Commun. Mass Spectrom.* **6**, 303 (1992).
106. K. A. Boering, J. Rolfe and J. I. Brauman, *Int. J. Mass Spectrom. Ion Processes* **117**, 357 (1992).
107. S. A. Lee, C. Q. Jiao, Y. Huang and B. S. Freiser, *Rapid Commun. Mass Spectrom.* **7**, 819 (1993).
108. A. J. R. Heck, L. J. de Koning, F. A. Pinske and N. M. M. Nibbering, *Rapid Commun. Mass Spectrom.* **5**, 406 (1991).
109. M. W. Senko, J. P. Speir and F. W. McLafferty, *Anal. Chem.* **66**, 2801 (1994).
110. E. M. Marzluff, S. Campbell, M. T. Rodgers and J. L. Beauchamp, *J. Am. Chem. Soc.* **116**, 6947 (1994).
111. E. M. Marzluff and J. L. Beauchamp, in *Proceedings of the 42nd ASMS on Mass Spectrometry and Allied Topic.*, Chicago, IL, May 29–June 3, 1994, p. 801.
112. A. G. Marshall, T. L. Wang and T. L. Ricca, *Chem. Phys. Lett.* **105**, 233 (1984).
113. R. G. Cooks, G. L. Glish, R. E. Kaiser, Jr, and S. A. McLuckey, *Chem. Eng. News* **69**, 26 (1991).

